Spectrum Journal of Innovation, Reforms and Development
Volume 38, April 2025 | ISSN (E): 2751-1731
WEBSITE: WWW.SJIRD.JOURNALSPARK.ORG

THERMAL PERFORMANCE OF AL2O3-H2O FLOW IN PIPES: A SIMULATION OF DOUBLE TWISTING TAPE WITH AND WITHOUT W-CUTTING

Intisar Rasheed Saleh 1,2
Karbala Technical Institute (1), Al-Furat Al-Awsat Technical University (2), 56001, Karbala, Iraq
Corresponding author: intisarkhursan@atu.edu.iq,

Abstract
This work predicts transfer of heat and drop in pressure of a fluid by simulated a flow in a pipe that has been installed employing double twisted tapes with two cases: with and without cutting. Where two tested fluid that flowing (H2O and Al2O3-H2O). The tests were conducted by applying Re number as a measure of the fluid's velocities, which range from 10000 to 35000. The impact of the presence of the cutting in twisting- tapes and the impact of nanoparticles on improving performance and heat transfer were tested. At the same time, it was determined whether the presence of the pipe with double twisting-tapes has a significant effect on its addition in the presence or absence of nanoparticles. As for the findings of the testing, the pipe with double-twisting tapes with nanofluid flow case expresses a transfer's heat more effectively than the smooth case; where when using nanoparticles in a pipe with double twisting-tape (φ = 0.02, 0.04, and0.06) at Re=10,000, the performance exceeds 1.74 at φ =0.06 for the case of w-cutting tapes. This indicates that, from the perspective of fluids and heating that transfer, employing a pipe with double twisting tape with cutting and adding nanoparticles is acceptable. As for friction factor values, φ = 0.06 case gives the higher amount of friction factor for all the velocities and for the two cases specially at w-cutting twisted tapes case.

Keywords: Twisted tape, w-cutting turbulent flow, thermal performance, nanofluid.

Introduction

The improved heat transfer approach is now being used to raise the thermal applications performance while saving material and energy. By implementing these strategies, it is possible to reduce the size and operating expenses [1–3]. Optimizing the transmission of heat is a key concern for energy saving and advantageous from an economic perspective. Effective techniques for enhancing heat transfer include the employment of passive devices such as wire inserts, roughness elements, twisted tapes, etc. Even though there are numerous approaches for better transfer of heat in thermal and technical applications, twisting-passages and twisting tapes have traditionally been employed in tube and shell construction to enhance passive heat transmission, heat exchangers,

and fluid transfer pipes, solar water and air heaters, power stations, and air conditioners are some examples of the many thermal applications. The devices insertion are easy to manufacture, replaceable, and quick to remove for maintenance. Numerous experiments have been conducted on various twisted tape shapes to speed up heat transmission [4-8]. Several correlations were developed to determine the behavior and the flowing characteristics associated with the insertion of twisting- tapes. The current research reviews earlier studies on the application of twisting-tapes to boost heat transmission. Previous experimental and numerical studies on various types of twisting-tapes were examined based on the literature review [9-11].

Eiamsa et al. [12] analyze several twisting-tapes in various configurations and TiO_2 in various amounts to improve the thermal-performance features in a tube. The performance factor, up to 1.45, was the result of usage. The thermal performance was greater when water containing TiO_2 nanoparticles was employed with H_2O. In addition, by simulation, Hosseinnezhad [13] inserted twin-twisting tapes into a heat exchanger to test the turbulent passage of Al_2O_3-water. The current study's examined characteristics include Re numbers between 10,000 and 30,000 and the impact of the twisting-tapes inserts' twist-ratio between 2.55 and 4.0. According to the study's findings, the average (Nu) rises when the twisting- ratio, and volume percentage of Al_2O_3 nanoparticles in the fundamental fluid are reduced. The highest performance evaluation criterion values are 1.6 and 1.5for twist ratios of 3.25 and 2.5respectively. Bhuiya et. al. [14] investigated the effects of employing twisted tapes on the thermal system. According to the experiment, the twisted tape produced more swirling flow, which in turn caused the thermally boundary layers along the streamlining to be disturbed more effectively, ultimately resulting in the maximum heat that transfered. In another experiment, the greatest perforation resulted in less swirling, whereas a smaller perforation yielded less fluid flow agitation. Wei [15] examined the heat transmission and flow of a CuO-H_2O in a conduit at different concentration (1–4%). The simulations were run in the with varying with Reynolds values between 3000 and 36,000. Researchers have investigated the impacts of employing a CuO-water nanofluid. Based on the data, the tube's optimal efficiency coefficient is 2.1 when Re = 36,000 and φ = 4%. Rahimi et. al. [16] compared the findings of several modified types of twisting- tapes: Notched, jagged, and punctured. Their outcomes indicated that the jagged type achieved the optimal (Nu). In comparison, the classic twisting- tape ranked second, following by the notched and puncture. The jagged twisted tape demonstrated a maximum rise of 31% in the (Nu)compared to the classic twisting- tape. Moreover, according to Sundar et al. [17], who computed the convective transport of heat of a Fe3O4-water, the friction factor and (Nu) were improved by 10.0% and 30.5%, respectively, at 0.6% volume concentration when compared to water under similar operating conditions. When water and carbon nanotubes (CNTs) were mixed in a horizontal tube with a Reynolds number of 800 and a weight concentration of 0.5%, Ding et al. [18] saw a 345.0% rise in heat that transfered. Hashemi and Behabadi [19] made a nanofluids with varying concentrations of 0.5%, to 2.0%, they found that helically coiled tubes, as opposed to straight tubes, improved heat transfer the most. Convective heat transfer of CuO-H_2O with concentrations of 0.10%, to 0.30% was examined by Suresh et al. [20] and revealed (Nu)improvements of 6%, 10%, and 12.5%, respectively, in comparison to water. Also, To accelerate heat transmission in a simple tube, Al_2O_3 was utilized by Mashayekhi et al. [21] in conjunction with twisting- tapes equiping. It has been discovered that, in comparison to a plain tube, heat transfer and friction factors significantly rise when twisting tape is equipped in a pipe.

This is explained by the flow pattern's conical tornado-shaped structures forming, which improves flow mixing. According to the outcomes gained by Esmaeilzadeh et al. [22], using the thicker twisting-tape inserts improves the heat transmission of the nanofluids. The air flow properties inside the pipe with double twisting- tape were investigated by Bhuiya et al. [23]. They demonstrated how decreasing porosity raises the friction factor and (Nu). Additionally, their findings indicated that the optimum enhancement in heat transport was approximately 290%. The goal of this work is to find the highest possible thermal performance using twisted tapes (with and without w-cutting) in the presence of nanofluids, which in turn helped to increase heat transfer. In our current work, double-twisting- tapes were inserted into the testing pipe to examine the effects of three distinct concentrations (0.02, 0.04, and 0.06) of the nanofluid (Al_2O_3-water) that were examined and contrasted with water as a fluid. simulation was carried out to find that, in addition to a large rise in pressure drop during flow, the enhancement of thermal performance improved as these concentrations rise and with Appling the case of w-cutting twisted tapes.

2. NUMERICAL ANALYSIS

2.1 Model Description

The geometry of typical pipes is designed with and without double twisted tape. The investigation tested the impact of cutting the tapes with w-cutting shape (as in figure 2), as table 1 illustrates. The working fluid used is Al_2O_3-H_2O with three nanoparticle volume fractions: 0.0%, 2.0%, and 4.0%. The nanoparticle size is 75 nm. Table 2 provides the characteristics of the fluid. All tests are conducted under uniform heat flux conditions applied to the pipe. The study considers a specific range of fluid velocities, using the Reynolds number (Re) as the basis for selecting velocities, with Re values ranging from 10^4 to 3.5×10^4. Figure 1 illustrates the details of geometry.

Table (1) The dimensions of the testing sections

Parameter	**Symbol**	***dimensions***
Pipe length	L	960mm
Inner diameter	D_i	26 mm
Outer	D_o	30 mm
diameter	t	4.0 mm
Tube thickness	e	
		10.0 mm
Cut width	w	
	h	
Tape width	y	23.0 mm
Height of cut		4 mm
Tape pitch		110 mm

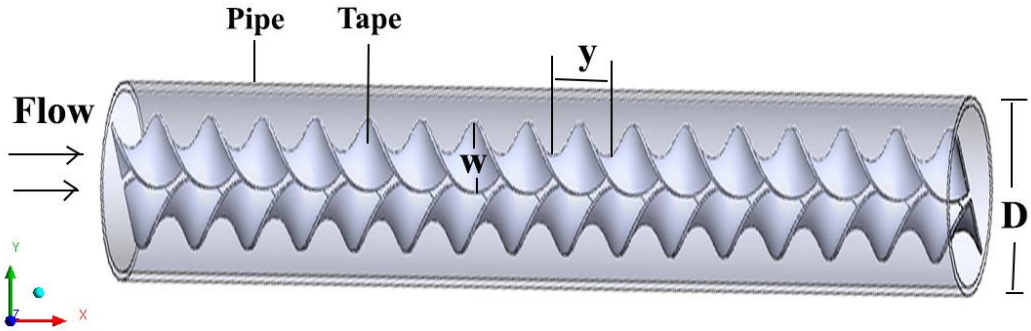

a.The details of the pipe

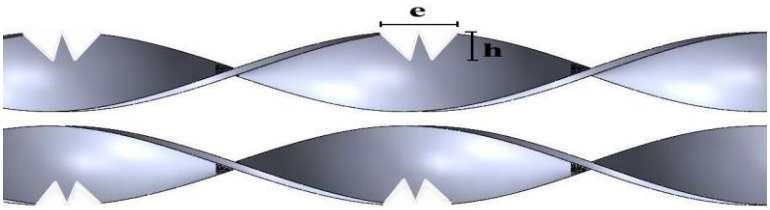

b.The details of the twisted and w-cut

FIGURE1 the schematic diagram of the pipe

Table (1) Thermo-physical properties of (H_2O)and solid nanoparticles(Al_2O_3)[24].

Material	*ρ.(kg/m^3)*	*Cp.(J/kg K)*	*k.(W/m K)*
Pure water	997.1	4179	**0.613**
Al_2O_3	1003	531.8	**76.5**

The values in Table 1 for each volume fraction evaluated in this work are computed using the following formulae. The literature follows the same equation convention [25]. The associated equations reflect: density, viscosity and the thermal conductivity. Symbols and subscripts are explained in the terminology section. Tables were used to select fixed property values for the fluid mixture's 300 K inlet temperature.

$$\rho_{nf} = (1-\varphi)\,\rho_{bf} + \varphi\,\rho_p \quad (1)$$

$$(\rho C_p)_{nf} = (1-\varphi)\,(\rho . C_p)_{pf} + \varphi(\rho C_p)_p \quad (2)$$

$$\mu_{nf} = \mu_{pf}\,(1+2.5\,\varphi) \quad (3)$$

$$k_{np} = \frac{k_p+2k_{bf}+2(k_p-2k_{bf})\varphi}{k_p+2k_p-2(k_p-2k_{bf})\varphi}\,k_{bf} \quad (4)$$

2.2 Governing equations

This model's hypothesis posits a turbulent, three-dimensional, incompressible flow in which gravity's influences are disregarded. The continuity, momentum, and energy equations [26] are the equations that govern in the fluid region. They are expressed as

:

Continuity equation [26]:

$$\frac{\partial U}{\partial x}+\frac{\partial V}{\partial y}+\frac{\partial W}{\partial z}=0 \quad (1)$$

Momentum equations for 3 coordinates(x, y, and z) [26]:

$$\rho\left(\frac{\partial u^2}{\partial x}+\frac{\partial uv}{\partial y}+\frac{\partial uw}{\partial z}\right)=-\frac{\partial P}{\partial x}+\frac{\partial}{\partial x}\left(2\mu_{eff}\frac{\partial u}{\partial x}\right)+\frac{\partial}{\partial y}\left(\mu_{eff}\frac{\partial u}{\partial y}\right)\frac{\partial}{\partial z}\left(\mu_{eff}\frac{\partial u}{\partial z}\right)+\frac{\partial}{\partial y}\left(\mu_{eff}\frac{\partial v}{\partial x}\right)+\frac{\partial}{\partial z}\left(\mu_{eff}\frac{\partial w}{\partial x}\right) \quad (2)$$

$$\rho\left(\frac{\partial vu}{\partial x}+\frac{\partial v^2}{\partial y}+\frac{\partial vw}{\partial z}\right)=-\frac{\partial P}{\partial y}+\frac{\partial}{\partial x}\left(\mu_{eff}\frac{\partial v}{\partial x}\right)+\frac{\partial}{\partial y}\left(2\mu_{eff}\frac{\partial v}{\partial y}\right)+\frac{\partial}{\partial z}\left(\mu_{eff}\frac{\partial v}{\partial z}\right)+\frac{\partial}{\partial x}\left(\mu_{eff}\frac{\partial u}{\partial y}\right)+\frac{\partial}{\partial z}\left(\mu_{eff}\frac{\partial w}{\partial y}\right) \quad (3)$$

$$\rho\left(\frac{\partial wu}{\partial x}+\frac{\partial wv}{\partial y}+\frac{\partial w^2}{\partial z}\right)=-\frac{\partial P}{\partial z}+\frac{\partial}{\partial x}\left(\mu_{eff}\frac{\partial w}{\partial x}\right)+\frac{\partial}{\partial y}\left(\mu_{eff}\frac{\partial w}{\partial y}\right)+\frac{\partial}{\partial z}\left(2\,\mu_{eff}\frac{\partial w}{\partial z}\right)+\frac{\partial}{\partial x}\left(\mu_{eff}\frac{\partial u}{\partial z}\right)+\frac{\partial}{\partial y}\left(\mu_{eff}\frac{\partial v}{\partial z}\right) \quad (4)$$

energy equation [27] :

$$\frac{\partial uT}{\partial x}+\frac{\partial vT}{\partial y}+\frac{\partial wT}{\partial z}=\frac{\partial}{\partial x}\left(\Gamma_{eff}\frac{\partial T}{\partial x}\right)+\frac{\partial}{\partial y}\left(\Gamma_{eff}\frac{\partial T}{\partial y}\right)+\frac{\partial}{\partial z}\left(\Gamma_{eff}\frac{\partial T}{\partial z}\right) \quad (5)$$

$\Gamma_{eff=}\ \Gamma+\Gamma_t$

$\Gamma t=\frac{v_t}{\sigma_t}$, σ_t is the turbulent Prandtl number.

The standard (k-ϵ)model, a popular semi-empirical turbulence model, is used to represent turbulence in the flow. Two equations are utilized in this method: one for the transfer of turbulent kinetic energy (k) and another for the disintegration of turbulence kinetic energy (ϵ).

For turbulent kinetic energy (***k***)[28]:

$$\rho\left(\frac{\partial}{\partial x}(ku)+\frac{\partial}{\partial y}(kv)+\frac{\partial}{\partial z}(kw)\right)=\frac{\partial}{\partial x}\left(\frac{\mu_t}{\sigma_k}\frac{\partial k}{\partial x}\right)+\frac{\partial}{\partial y}\left(\frac{\mu_t}{\sigma_k}\frac{\partial k}{\partial y}\right)+\frac{\partial}{\partial z}\left(\frac{\mu_t}{\sigma_k}\frac{\partial k}{\partial z}\right)+G-\rho\varepsilon \quad (6)$$

For energy dissipation rate (**ε**)[29]:

$$\rho\left(\frac{\partial}{\partial x}(\varepsilon u)+\frac{\partial}{\partial y}(\varepsilon v)+\frac{\partial}{\partial z}(\varepsilon w)\right)=\frac{\partial}{\partial x}\left(\frac{\mu_t}{\sigma_\varepsilon}\frac{\partial \varepsilon}{\partial x}\right)+\frac{\partial}{\partial y}\left(\frac{\mu_t}{\sigma_\varepsilon}\frac{\partial \varepsilon}{\partial y}\right)+\frac{\partial}{\partial z}\left(\frac{\mu_t}{\sigma_\varepsilon}\frac{\partial \varepsilon}{\partial z}\right)+C_{1\varepsilon}\,\rho\,\frac{\varepsilon}{k}\,G-C_{1\varepsilon}\,\rho\,\frac{\varepsilon}{k} \quad (7)$$

Where G is referred to as the generation term and is given [30]:

$$G=\mu_t\left[2\left(\frac{\partial u}{\partial x}\right)^2+2\left(\frac{\partial v}{\partial y}\right)^2+2\left(\frac{\partial w}{\partial z}\right)^2+\left(\frac{\partial v}{\partial y}\frac{\partial u}{\partial x}\right)^2+\left(\frac{\partial v}{\partial z}\frac{\partial w}{\partial x}\right)^2+\left(\frac{\partial v}{\partial z}\frac{\partial w}{\partial y}\right)^2\right] \quad (8)$$

According to [28], $q_{convection}$, or the convective flux of heat is as follows:

$$q_{convection=}\quad m^{\circ}\quad c_p\quad (\quad T_{out}\quad -\quad T_{in}\quad) \quad (9)$$

The mean heat transfer coefficient(h) can be found by the following [31]:

$$h=\frac{q_{conv}}{(T_w-T_b)} \quad (10)$$

Where the mean wall temperature is calculated by [32]:

$$T_w=\frac{1}{n}\sum T_{wn} \quad (11)$$

Mean bulk temperature (T_b) is determined by [33]

$$T_b = \frac{\int_0^L \int_0^H \int_0^W \rho\ c_p\ uT\ dx\ dy\ dz}{\int_0^L \int_0^H \int_0^W \rho\ u\ dx\ dy\ dz} \quad (12)$$

The mean Nusselt number was first presented.

$$Nu = \frac{h\ .D_h}{k} \quad (13)$$

Darcy-Weisbach expression is employed to define the friction factor(f) as [34].

$$f = \frac{\Delta P\ .D_h}{\frac{1}{2}\rho\ U_{avg}^2\ .\ L} \quad (14)$$

The overall performance factor (η) [34]:

$$\eta = (Nu/Nu_0)/(f/f_0)^{1/3} \quad (15)$$

2.3 Boundary conditions

The equations are meant to be solved by applying boundary conditions to the boundaries of the numerical domain as in Table(3)

Table (3) The simulation's boundaries

Boundary Ends	The boundary conditions
Inlet	T_{in}=305K, Re=10000-35000
Outlet	($\partial u/\partial x = \partial v/\partial y = \partial w/\partial z = 0$), zero gauge.-pressure is mentioned at the outlet domain
Surfaces	the velocity is taken to be zero (no slip) , u=0, v=0, w=0, $\partial P/\partial n = 0$, where n is a normal unit

2.4 Mesh Generation Grid independence

Grids play a crucial role in mesh generation, with quad grids used to cover the tube and regions within the flow field. To improve mesh quality near walls where velocity and temperature gradients are more pronounced, boundary layer meshes are applied to the inner surfaces of the pipe and to the twisting- tapes. For the rest of the flow domain, curvature grids are employed. The final grid configuration is shown in Figure 2. Grid independence tests are performed at (Re) of:10,000 for the smooth pipe, the pipe with twisting- tapes only and the pipe with cutting twisted tapes to evaluate the Nu and f values, as summarized in Table 3.

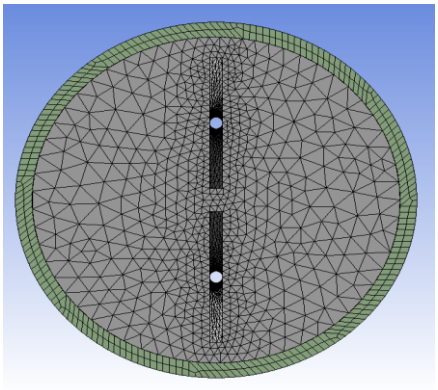

FIGURE. 2 The considered mesh generation

Table (3) Different grids and their (Nu)and(f)for different tested cases at Re= 10,000.

Case	No. of grid elements	Nu	*f*
Smooth pipe	517,223	28.227	0.0793
	611,107	29.042	0.0882
	684,646	30.328	0.0925
	754,487	30.331	0.0933
Pipe fitted with twisted tapes	3,174,431	77.953	0.103
	3,321,562	78.521	0. 132
	3,552,312	79.44	0. 174
	3,868,884	79.444	0.18
Pipe fitted with twisted tapes with w-cut	2,622,331	84,322	0.13
	2,789,887	85,432	0.15
	3,126,478	88,489	0. 195
	3,232,455	88,543	0. 211

3. RESULTS AND DISCUSSION

After adding and testing a variety of characteristics influencing heat transfer and pressure change, a simulation of the flow in a pipe is carried out to evaluate its performance. The tube's thermal performance is enhanced by the addition of double-twisted tapes inside with two cases: with and without w-cutting of twisted tapes. Further, the flowing water is treated with one of the highly conducting nanoparticles (Al_2O_3), which is then evaluated at various volume fractions (0.02, 0.04, and 0.06) to see which one best enhances overall performance.

Numerous investigations have been carried out to ascertain the impact of adding two tapes. Regarding the Nusselt number, the figure 4 and 5 illustrates that, in every investigated case, heat transmission rises as fluid velocity rises. As the Rey number rises, the fluid's velocity and momentum rise, allowing it to absorb more heat from the tube wall, causing the temperature differential between the fluid's bulk and tube wall to decrease, and ultimately results in a rising in the (Nu).

In figures 4 and 5, the cases are particularly evident in the instance where the nanofluid was employed with the twisting- tapes present and by a highest (0.06), which means that it rises in (Nu)by around 53% over the smooth pipe case. The rise appears more clearly and higher when comparing the w-cut case with the smooth pipe, it rises in Nusselt number by around 60%

The liquid and nanoparticles react differently when there are twisted tapes involved because they alter the velocity distribution. Further, examining the impact on adding nanoparticles to the foundation fluid and the presence of multiple twisting- tapes at a constant (Re) reveals that the affectability of nanoparticles and the presence of twisted tape become more significant as (Re)boosts and the volume fraction of nanoparticles rises. In general, Adding twisted tape rises (Nu) by: Enhancing fluid mixing and boundary layer disruption, inducing swirl flow and secondary vortices, raising effective thermal conductivity and velocities and providing additional transferring in heat at the surface area.

The effect of w-cutting in the tapes will cause the flow behind it to be cut off, thus generating strong vortices, flow separation, and thermal boundary layer break up. All of this, in turn, causes greater mixing of the fluid and thus greater heat transfer. Adding nano-materials enhances (Nu)

by: Boosting thermal conductivity of the followed fluid, rising Brownian motion & thermo-apheresis, enhancing heat diffusion, Disrupting the boundary layer, reducing resistance to heat transfer, increasing heat capacity, allowing better heat absorption and inducing secondary flows, leading to better mixing.

Figures 6 and 7 show the (friction factor) as a function of the volume fraction of the (Re)within a pipe containing two twisted tapes with and without w-cutting. Examining how the twisted tape affects flow direction reveals that its presence boosts the friction factor; at Re = 10,000, twisting-tape raises the friction factor by 2.1 and 1.6 times for cases with and without w-cutting respectively as compared to smooth pipe under the same circumstances, that is due to flow resistance is boosted considerably by the tapes and w-cutting. The swirls and eddies create extra friction. In the other instances in Figures 6 and 7, the friction factor is greatly raising clearly by raising the volume percentage of nanoparticles. This problem arises because a greater Re number leads in a thinner boundary layer, which lessens the impact of the area of viscous, the gradient of velocities, and ultimately (*f*). The existence of nanoparticles rises fluid viscosity, and as the volume fraction rising, the (*f*) grows as well.

To more explain for this behavior we should note that adding nanomaterials increases the friction coefficient (f) due to: Higher viscosity, making the fluid more resistant to flow, raised wall shear stress from particle-fluid interactions, Momentum transfer & turbulence enhancement.Particle aggregation, obstructing flow and Surface roughness modifications leading to higher drag. As for Twisted tape inserting objective and its impact, Adding twisted tape increases the friction coefficient (f) due to: Longer helical flow path, increasing fluid-wall interaction, Induced swirl & turbulence, enhancing velocity gradients, Reduced flow area, leading to higher velocities.

Continuous boundary layer disruption, preventing stabilization, Vortex formation & eddies, increasing momentum transfer and Surface roughness & wake regions, adding extra drag.

In figures 8 and 9 The entire performance of the pipe has been established by analyzing the fluid's behavior, the impact of twisting- tape, and adding the nanoparticles to the water. The three figures clearly show a comparison based on the nanoparticles and the presence of twin twisting tapes. The best thermal-compressive performance was found at the case of channel fitted with W-cutting twisted tape, η=1.74 at Re=10000, demonstrated in the case of φ =0.06. Also, η=1.61 gained from the case of pipe with twisted tapes only at Re=10000.

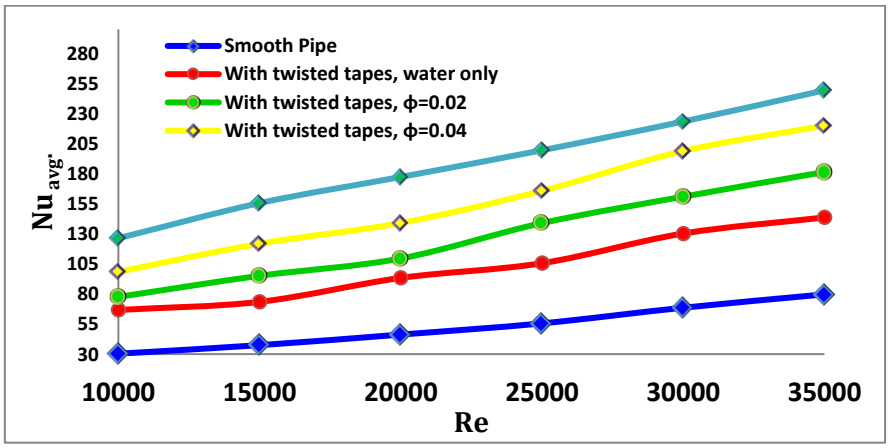

FIGURE 4 The relations of (Nu) with (Re) for pipe with twisted tape only, all tested cases volume fraction

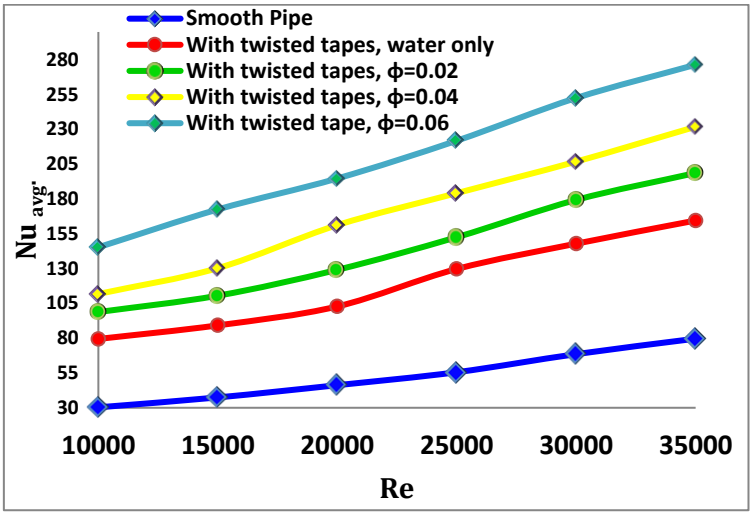

FIGURE 5 The relations of (Nu) with (Re) for the pipe with w-cutting twisted tape, all tested cases volume fraction

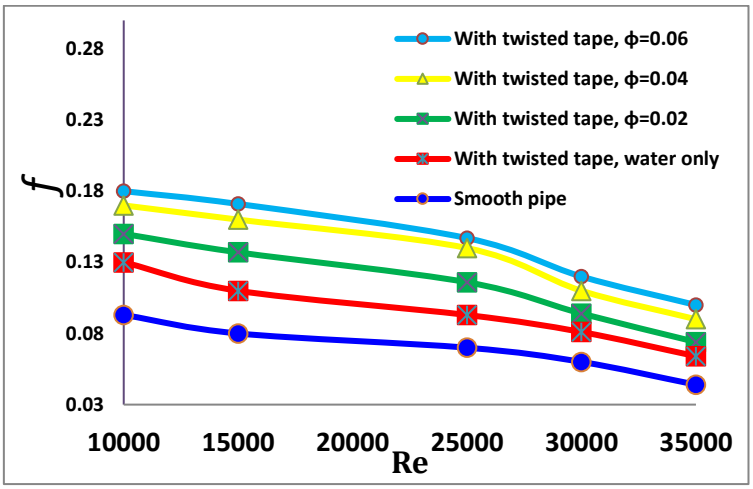

FIGURE 6 The relations of (*f*) with (Re) for the pipe with twisted tape only, all tested cases volume fraction

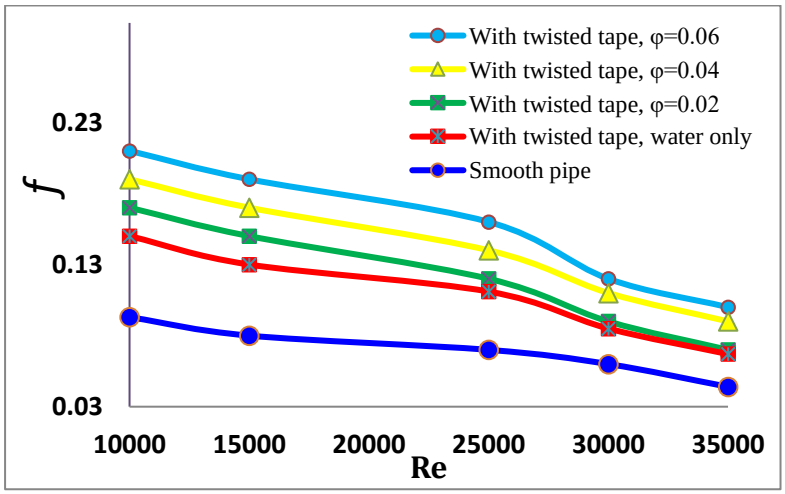

FIGURE 7 The relations of (*f*) with (Re) for the pipe with w-cutting twisted tape, all tested cases volume fraction

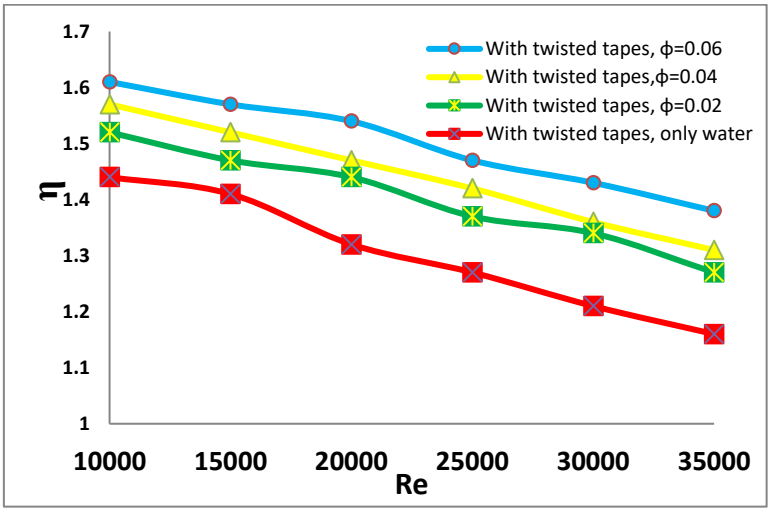

FIGURE 8 The relations of the performance with (Re) for the pipe with twisted tape only, all tested cases volume fraction

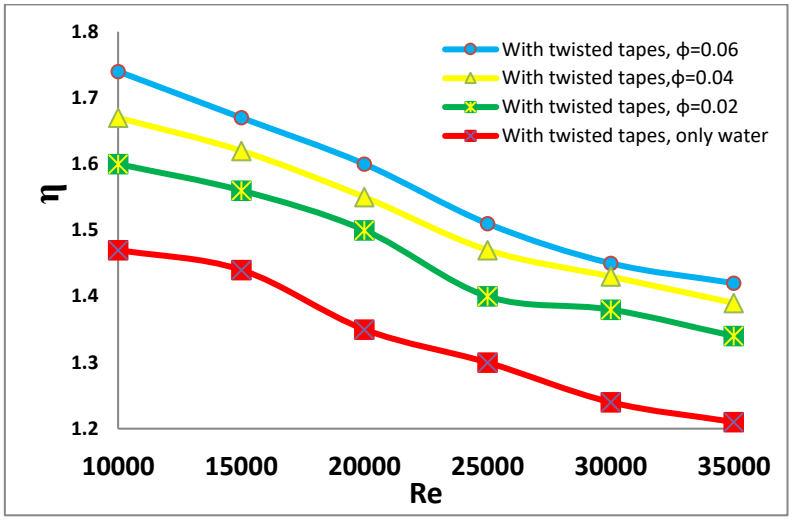

FIGURE 9 The relations of the performance with (Re) for the pipe with w-cutting twisted tape, all tested cases volume fraction

The relation between (Tw-Tb) as well as (Re) for the examples the findings of the w-cutting case was illustrated in Figure 10. As the (Re) varied from 10,000 to35,000,. the outcomes showed a significant drop in the amounts of (Tw-Tb) at the pipe with twisted tapes and Al_2O_3-H_2Ocase, where they ranged from 35.0 to 20.5. As the Re. number varied from 10,000 to 35,000, the case of smooth pipe obviously yielded the highest values of (Tw-Tb), which varied from 57.4 to 33.4. The case of (φ =0.06) with twisting the tape yields the optimal heat transmission when it is comparing to the remaining ratios because there is consistency in temperature and a raising in the amount of heat that transfered when the amount of (Tw-Tb) drops.

Regarding Figures 11, it illustrates how the Al_2O_3 that added to the water and the fitting of twisting tape with w-cutting affect the (Nu/ΔP) ratio for different values of (Re). According to the data, the case with the least values of (Nu/ΔP) for all Re number values is the pipe with the twisted tape and nanoparticles with φ =0.06. As the (Re) grew from 10,000 to 3,5000, the ratio varied between 16.5 and 2.52. The largest amounts of (Nu/ΔP) for all (Re) values are found in cases with smooth pipes

that run through pipes equipped with twisting tape and for water. This discrepancy results from the variance of the (Nu) in each case up to the variation in the heat that transferred in each case, where the case with φ =0.06 has the highest rate of heat transfer and the case with only water flowing has the lowest rate. Additionally, due to the variation in the pressure drop, which rises in each case with a raising in heat transfer and water velocity.

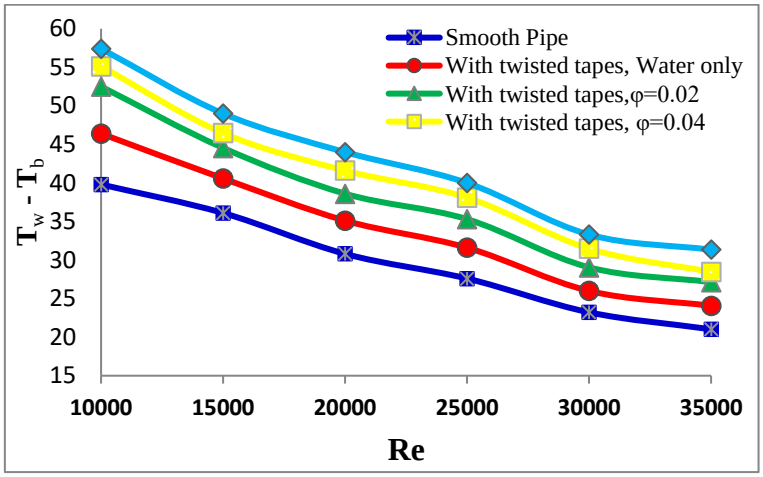

FIGURE 10 The relations of (T_w – T_b) for the pipe with w-cutting twisted tape, all tested cases volume fraction

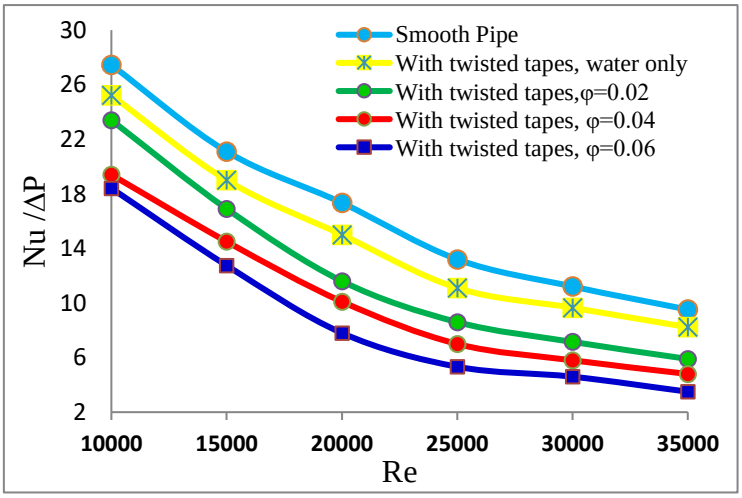

FIGURE11 The relations of (Nu/ΔP)with Re for the pipe with w-cutting twisted tape, all tested cases volume fraction

This section examines flow physics qualitatively by presenting qualitative findings, such as velocity distribution and velocity vectors. Figures 12, 13, and 14 show two distinct flowing fluids at Re values from 10,000 to 35,000 in latitude parts with velocity dispersion in a pipe with twin twisting tapes in two cases : with and without w-cutting. The flow in the twisting tape region became unstable and erratic due to the varying in the geometries. Due to the increased water velocity, which exacerbates turbulence and obstructs flow, irregularities and turbulence are evidently higher in case (b) than in case (a). These statistics indicate that the flow becoming

rotational in a pipe with twisting- tape at both the cases without the formation of vortices on the tapes .

In the case of multiple twisting- tapes on the direction of fluid flow, the flow's velocity profile and the velocity boundary layer's arrangement are altered by colliding with the twisted tapes, making the flow compatible with the tapes' shape and, as a result, producing vortices. These statistics indicate that the flow becoming rotational in a pipe with double-twisted tape at both cases specially at the case of w-cutting twisted tapes which generates more complex flow patterns and creates additional local circulation areas.velocity vectors usually demonstrate a noticeable shift with axial location along the pipe in Figures 8 and 9 demonstrates the strong swirling model for greater axial distance, which causes the angular momentum to increase for a = 200 mm, b = 400 mm, and c = 700 mm.

At figures (a, b, and c), the influence of angular momentum diminishes, weakening the process and intensity of creating swirling.

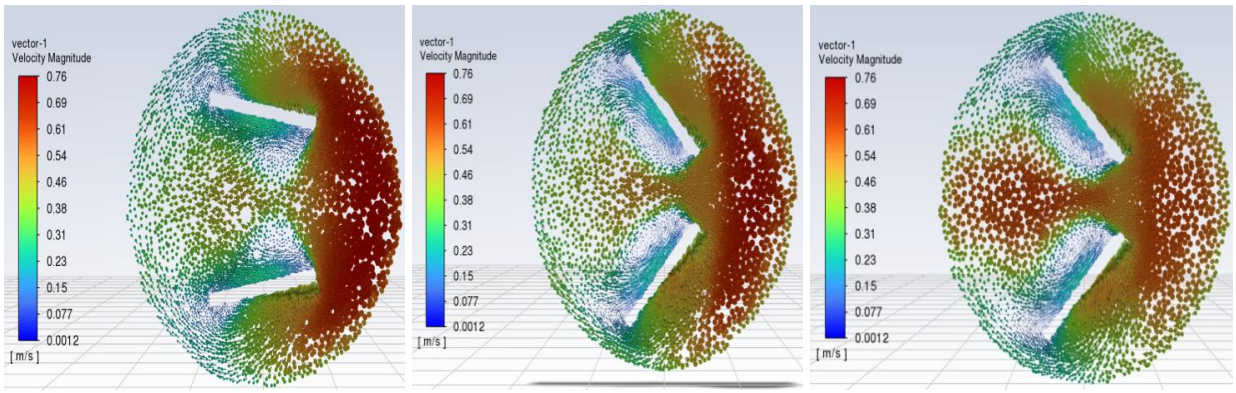

a.300 mm b.500 mm c. 700mm

FIGURE12 Velocity vectors of pipe fitted with twisted tape only, Al_2O_3-H_2O flow, φ =0.06, Re=10000

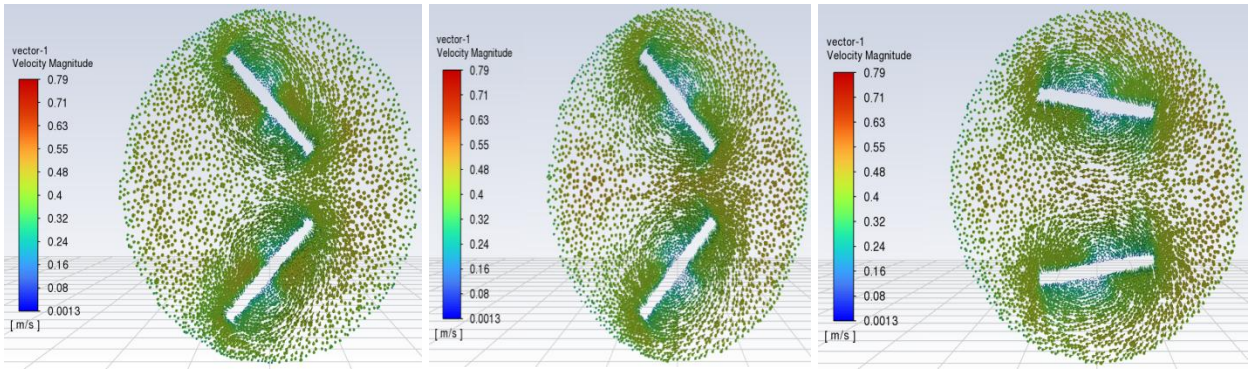

a.300 mm b.500 mm c.700 mm

FIGURE13 Velocity vectors of pipe fitted with w-cutting twisted tape, Al_2O_3-H_2O flow, φ =0.06, Re=10000

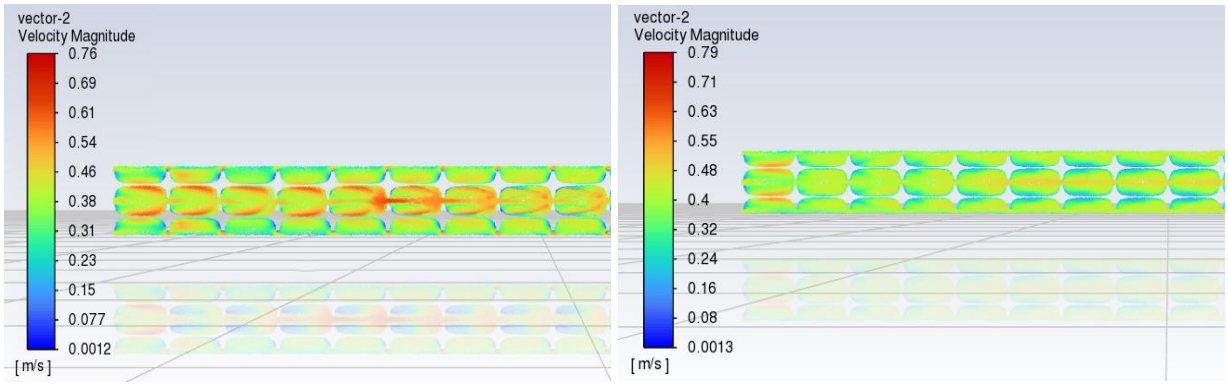

a.twisted tapes only b.cutting twisted tapes

FIGURE 14 The velocity vectors of the pipe two cases

The pressure drop difference between the two tested cases(with and without w-cutting) in the instance of a nano-flowing fluid with a concentration of 6 is depicted in figures 15 and 16. Exhibit the pressure reduction in the two tested pipes. In the case of w-cutting, demonstrate that the rate of pressure fall is evident.

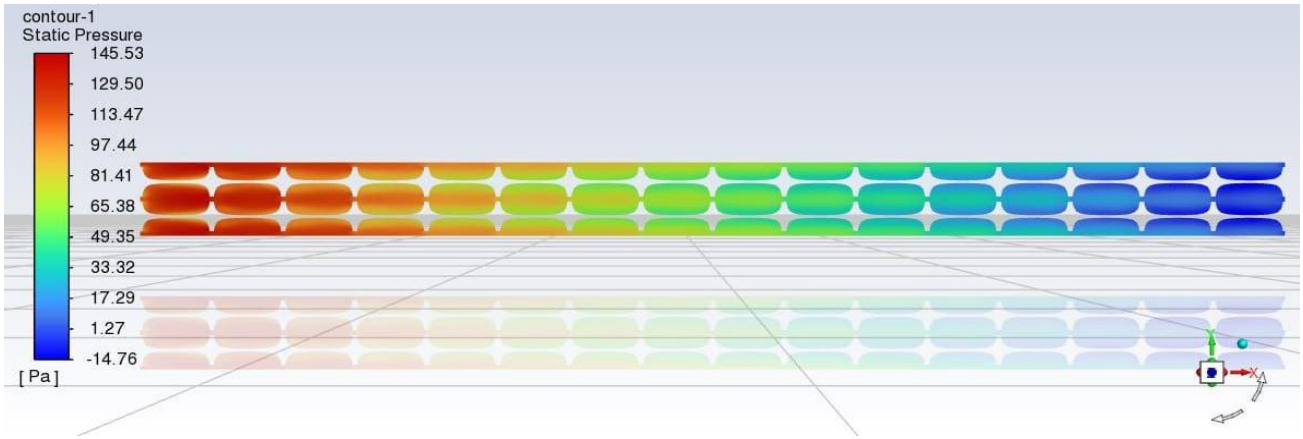

Figure 15 Presure contour of pipe for Al_2O_3-H_2O nanofluid, φ =0.06 at Re=10,000, twisted tapes only

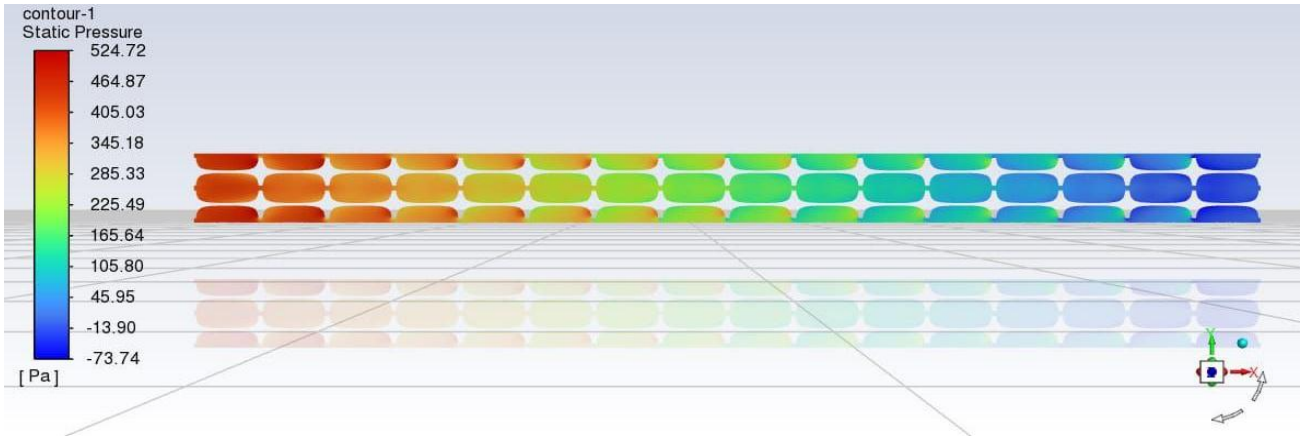

Figure16 Presure contour of pipe for Al_2O_3-H_2O nanofluid, φ =0.06 at Re=10,000, w-cutting twisted tapes

By contrasting the current study's results with those of Eiamsa-ard et al. [35] for a pipe with twin twisting- tape that has a width of 9.0 mm and a length of 1.0m, the current numerical approach is validated. The Nusselt number for the current experiment and the findings of Eiamsa-ard et al. [35] is shown in Figure 17 as a Reynolds number. The current numerical method's results clearly show strong agreement with the data collected from experiments (highest error is approximately 9%). Therefore, the numerical model that applied in this work has a respectable level of accuracy, making the numerical approach legitimate.

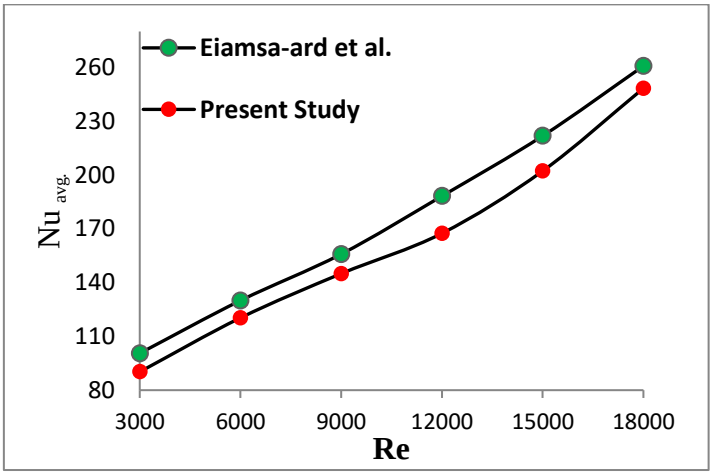

Figure 17 Validation between the current study and Eiamsa-ard et al. [35]

CONCLUSION

The current study utilizes numerical simulation to examine the heat that transferred of turbulent flow of nanofluid in a tube with double twisting- tapes. The outcomes collected show that:
-The (Nu) improves as the (Re)rises. The (Nu)rises by up to three times in the water flowing in the pipe(with twisting tapes) at Re = 10,000, and by up to 155 in the flow at Re = 35,000 in the pipe with two twisted tapes and Al_2O_3-H_2O with φ =0.06.
- The (Nu)of a pipe with two twisting tapes is significantly better than that of a plain pipe.
- From the viewpoint of fluids and heat that transferring, using a stream with twin twisting- tapes with w-cutting for water flow is appropriate because the performance is greater than 1.
- when using nanoparticles in a pipe with double twisting tape (φ = 0.02, 0.04, and0.06) at Re=10,000, the performance exceeds 1.61 at φ = 0.06, and equal to1.76 at w-cutting twisted tapes and these out comes decrease when the volume fraction of nanoparticle decrease. This indicates that, from the perspective of fluids and heat transfer, employing a pipe with double twisting tape and adding the nanoparti4les is acceptable.
- The friction factor in the pipe (without twisting- tapes) is 0.093 at (Re) 10,000 and 0.04 when it rises to 35,000. Examining how the twisted tape affects flow direction reveals that its presence boosts the friction factor; at Re = 10,000, twisted tape case and w-cutting twisted tapes case raises the friction factor by 1.7 and 2.3 times respectively compared to plain pipe under the exact circumstances
- There is a raise in performance in a pipe with twisting tape at both cases(with and without cutting) specially at the case of w-cutting twisted tapes which generates more complex flow patterns and

creates additional local circulation areas, that's help to make a good mixing and good heat transferring.

NOMENCLATURE

A	Surface area, m^2
D_h	Hydraulic-diameter ,m
e	width of the cut ,m
F	Friction. factor
H	The mean heat. Transfer coefficient. W/m^2K
h	Height of cut, m
K	thermal conductivity, W/m k
L	length of duct, m.
Nu	mean. Nusselt number
P	Tape pitch, m
Δp	fluid pressure-drop of duct, pa
q_{conv}	The convective heat flux. W/m^2.
Re	fluid Reynolds number
T	pipe thickness, m
$T_{w.}$	wall. temperature, K
$T_{in.}$	fluid Inlet temperature. K.
T_{out}	fluid outlet temperature. K.
W	Tape width, m
y	pitch of the tape, m
η	The overall heat performance
ρ	density, kg/m^3
φ	volume fraction of the nano-particles

REFRENCES

1. Li, Jintao, et al. "Effects of deformed twisted tapes on thermal performance enhancement of hydrogen fueled micro combustor for micro-thermophotovoltaic system." *Applied Thermal Engineering* (2025): 125413. https://doi.org/10.1016/j.applthermaleng.2025.125413
2. Shelare, Sagar D., Kapil R. Aglawe, and Pramod N. Belkhode. "A review on twisted tape inserts for enhancing the heat transfer." *Materials Today: Proceedings* 54 (2022): 560-565. V. Deviboga and S. Jayavel , "Numerical Simulation of heat transfer in channel with different ribs" vol.2 . 2320-2092. https://doi.org/10.1016/j.matpr.2021.09.012.
3. Marzouk, S. A., et al. "Enhancing heat transfer in a double-tube heat exchanger using perforated twisted tape and nanofluid." *Journal of Thermal Analysis and Calorimetry* (2025): 1-15. https://doi.org/10.1007/s10973-024-13930-x.
4. Nashee, S., & Mushatet, K. (2024). Performance study on turbulent heat transfer using rectangular air duct integrated with continuous and intermittent ribs turbulators. Thermal Science, 00, 214. https://doi.org/10.1108/WJE-06-2023-0233.
5. Chammam, Wathek, et al. "Estimation of heat transfer coefficient and friction factor with showering of aluminum nitride and alumina water based hybrid nanofluid in a tube with

twisted tape insert." *Scientific Reports* 13.1 (2023): 23071. https://doi.org/10.1038/s41598-023-49142-w.

6. Radhi, Firas Abdulamir, et al. "Experimental analysis of a photovoltaic thermal collector utilizing a novel spring insert in a micro-fin absorber tube with twisted tape, nanofluid, and nanophase change material integration." *Applied Thermal Engineering* 269 (2025): 126128. https://doi.org/10.1016/j.applthermaleng.2025.126128.
7. Nashee, Sarah R. "Numerical Study for Fluid Flow and Heat Transfer Characteristics in a Corrugating Channel." International Journal of Heat & Technology 41.2 (2023). https://doi.org/10.18280/ijht.410213.
8. Azmi, W. H., et al. "Comparison of convective heat transfer coefficient and friction factor of TiO2 nanofluid flow in a tube with twisted tape inserts." *International* Journal of Thermal Sciences 81 (2014): 84-93. https://doi.org/10.1016/j.ijthermalsci.2014.03.002
9. Aravamuthan, Srikanth, et al. *Numerical and experimental investigation of in-cylinder swirl flow using twisted tape in diesel engines*. No. 2013-01-2793. SAE Technical Paper, 2013. https://doi.org/10.4271/2013-01-2793.
10. Nashee, S.R. "Enhancement of heat transfer in nanofluid flow through elbows with varied cross-sections: A computational study". International Journal of Heat and Technology, Vol. 42, No. 1, pp. 311-319. 2024.

https://doi.org/10.18280/ijht.420133.

11. Hosseinnezhad, Rahim, et al. "Numerical study of turbulent nanofluid heat transfer in a tubular heat exchanger with twin twisted-tape inserts." *Journal of Thermal Analysis and Calorimetry* 132 (2018): 741-759. https://doi.org/10.1007/s10973-017-6900-5.
12. Eiamsa-ard, Smith, and Kunlanan Kiatkittipong. "Heat transfer enhancement by multiple twisted tape inserts and TiO2/water nanofluid." *Applied Thermal Engineering* 70.1 (2014): 896-924. https://doi.org/10.1016/j.applthermaleng.2014.05.062.
13. Hosseinnezhad, Rahim, et al. "Numerical study of turbulent nanofluid heat transfer in a tubular heat exchanger with twin twisted-tape inserts." *Journal of Thermal Analysis and Calorimetry* 132 (2018): 741-759. https://doi.org/10.1007/s10973-017-6900-5.
14. Bhuiya MMK, Chowdhury MSU, Saha M, et al. Heat transfer and friction factor characteristics in turbulent flow through a tube fitted with perforated twisted tape inserts. *Int Commun Heat Mass Transf* 2013; 46: 49–57. https://doi.org/10.1016/j.icheatmasstransfer.2013.05.012.
15. He, Wei, et al. "Effect of twisted-tape inserts and nanofluid on flow field and heat transfer characteristics in a tube." International Communications in Heat and Mass Transfer 110 (2020): 104440. https://doi.org/10.1016/j.icheatmasstransfer.2019.104440.
16. Rahimi M, Shabanian SR, andAlsairafi AA. Experimental and CFD studies on heat transfer and friction factor characteristics of a tube equipped with modified twisted tape inserts. *Chem Eng Process Process Intensif* 2009; 48: 762–770. https://doi.org/10.1016/j.cep.2008.09.007.
17. Sundar, L. Syam, and K. V. Sharma. "Turbulent heat transfer and friction factor of Al2O3 nanofluid in circular tube with twisted tape inserts." *International Journal of Heat and Mass Transfer* 53.7-8 (2010): 1409-1416. https://doi.org/10.1016/j.ijheatmasstransfer.2009.12.016.

18. Ding, Yulong, et al. "Heat transfer of aqueous suspensions of carbon nanotubes (CNT nanofluids)." *International Journal of Heat and Mass Transfer* 49.1-2 (2006): 240-250. https://doi.org/10.1016/j.ijheatmasstransfer.2005.07.009.
19. Akhavan-Behabadi, M. A., et al. "Pressure drop and heat transfer augmentation due to coiled wire inserts during laminar flow of oil inside a horizontal tube." *International Journal of Thermal Sciences* 49.2 (2010): 373-379. https://doi.org/10.1016/j.ijthermalsci.2009.06.004
20. Suresh, S., M. Chandrasekar, and S. Chandra Sekhar. "Experimental studies on heat transfer and friction factor characteristics of CuO/water nanofluid under turbulent flow in a helically dimpled tube." *Experimental Thermal and Fluid Science* 35.3 (2011): 542-549. https://doi.org/10.1016/j.expthermflusci.2010.12.008
21. Mashayekhi, R., Arasteh, H., Talebizadehsardari, P., Kumar, A., Hangi, M., & Rahbari, A. (2021). Heat Transfer Enhancement of Nanofluid Flow in a Tube Equipped with Rotating Twisted Tape Inserts: A Two-Phase Approach. *Heat Transfer Engineering*, *43*(7), 608–622. https://doi.org/10.1080/01457632.2021.1896835
22. Esmaeilzadeh, E., et al. "Study on heat transfer and friction factor characteristics of γ-Al2O3/water through circular tube with twisted tape inserts with different thicknesses." *International Journal of Thermal Sciences* 82 (2014): 72-83. https://doi.org/10.1016/j.ijthermalsci.2014.03.005
23. Bhuiya, M. M. K., et al. "Heat transfer augmentation in a circular tube with perforated double counter twisted tape inserts." International Communications in Heat and Mass Transfer 74 (2016): 18-26. https://doi.org/10.1016/j.icheatmasstransfer.2016.03.001
24. Chokphoemphun, Suriya, et al. "Thermal performance of tubular heat exchanger with multiple twisted-tape inserts." Chinese Journal of Chemical *Engineering* 23.5 (2015): 755-762. https://doi.org/10.1016/j.cjche.2015.01.003.
25. Pushpa B V, Prasanna B M R, Younghae Do and M.Sankar" Numerical study of doublediffusive convection in a vertical annular enclosure with a baffle" IOP Conf. Series: Journal of Physics: Conf. Series 908 (2017). https://doi.org/10.1088/1742-6596/908/1/012081.
26. Nashee, Sarah Rabee, and Haiyder Minin Hmood. "Numerical Study of Heat Transfer and Fluid Flow over Circular Cylinders in 2D Cross Flow." Journal of Advanced Research in Applied Sciences and Engineering Technology 30.2 (2023): 216-224. https://doi.org/10.37934/araset.30.2.216224.
27. Rahman, A. (2023). Experimental Investigations on Single-Phase Heat Transfer Enhancement in an Air-To-Water Heat Exchanger with Rectangular Perforated Flow Deflector Baffle Plate. International Journal of Thermodynamics, 26(4), 31-39. https://doi.org/10.5541/ijot.1285385.
28. Nashee, S. R. (2024). Numerical Simulation of Heat Transfer Enhancement of a Heat Exchanger Tube Fitted with Single and Double-Cut Twisted Tapes. International Journal of Heat and Technology, 42(3), 1003–1010. https://doi.org/10.18280/ijht.420327.
29. Mushatet, Khudheyer, and Sarah Nashee. "Experimental and computational investigation for 3-D duct flow with modified arrangement ribs turbulators." Thermal Science 25.3 Part A (2021): 1653-1663.

30. Rahman, A., Dhiman, S. K. (2024). Thermo-fluid performance of a heat exchanger with a novel perforated flow deflector type conical baffles. Journal of Thermal Engineering, 10(4), 868-879. https://doi.org/10.14744/thermal.0000846.
31. Sarah Rabeea Nashee, Zainalabden A. Ibrahim, Dhoha Kamil. (2024). Numerical investigation of flow in vertical rectangular channels equipped with three different obstacles shape. AIP conference proceeding. Fourth International Conference On Advances In Physical Sciences And Materials: Icapsm 2023, 17–18 August 2023,Coimbatore, India. Volume 3122, Issue 1. https://doi.org/10.1063/5.0216016.
32. Kaplan, Sami, et al. "Innovative arrangement of circular angled fins for maximizing the discharge performance of triple-tube heat storage systems." *International Journal of Low-Carbon Technologies* 19 (2024): 938-951. https://doi.org/10.1093/ijlct/ctae014
33. Nashee, S. R. and Mushatet, K. S. (2025). Impact of Ribs with Multiple Arrangements on the Behavior of a Turbulent Flow in a Rectangular Channel. *Journal of Heat and Mass Transfer Research*, *12*(2), 259-270. https://doi.org/10.22075/jhmtr.2025.34713.1575.
34. Basher, Hadi O. "Enhancement of Heat Transfer and Fluid Flow Characteristics in an Elliptical Tube with a Twisted Tube Section and Twisted Tape Inserts: A Numerical Investigation." *International Journal of Heat & Technology* 42.4 (2024). 10.18280/ijht.420437
35. S. Eiamsa-ard, C. Thianpong, P. Eiamsa-ard, Turbulent heat transfer enhancement by counter/co-swirling flow in a tube fitted with twin twisted tapes, Exp. Therm. Fluid Sci. 34, (2010) 53-62. https://doi.org/10.1016/j.expthermflusci.2009.09.002.